Referee #2 - Eleanor Browne

Rivellini et al made ambient measurements of aerosol chemical composition with an SP-AMS on the campus of the National University of Singapore. PMF analysis was performed on the data and the authors investigated how the inclusion of rBC and metals into the PMF affected the interpretation of the PMF results. Overall, this is an interesting data set that highlights how rBC and metal measurements can enhance our understanding of aerosol sources.

Author's response: We thank for the positive comments from the reviewer. We have provided our point-to-point responses below (in blue colour) to address the questions/comments as shown below:

Major comments

1) The SP-AMS calibrations and data analysis need to be described in more detail. In particular, CE needs to be considered/discussed in more detail. Is there evidence for the morphology and coating of the rBC particles varying at all over the course of the measurements (and consequently a varying CE)? How would a varying CE affect the interpretation of the measurements and the PMF results?

Author's Response: We conducted four calibrations using ammonium nitrate and Regal black particles as described in the original manuscript. To ensure the quality of calibration, the inter-instrument comparisons have be conducted to show that our SP-AMS calibrations for both rBC and NR-PM are reasonable. The SP-AMS measurements were compared with other co-located measurements from an aethalometer (model AE33, Magee scientific), an OC/EC analyser (Sunset Laboratory) and a Monitor for AeRosols and GAses in ambient air analyzer (MARGA, Metrohm) over the sampling period.

Sulfate (SO_4^{2-}) and organic mass concentrations from the SP-AMS (CDCE-corrected) were compared to SO_4^{2-} and OM measured by the MARGA and the OC/EC analyser, respectively (Figure S3a and b in the revised SI). Aside from the good correlations that underline a good temporal response from all instruments, the slopes are in the range of 0.81-0.88, suggesting that the mass concentrations of SO_4^{2-} and organic measured by the SP-AMS are ~12-19% lower than those measured by the MARGA and the OC/EC analyser, respectively. This could be partially explained by the 1 µm cut-size of the SP-AMS, while the two other instruments were measuring $PM_{2.5}$.

The rBC mass concentrations (CE = 0.6) were compared with BC and EC measured by the aethalometer and the OC-EC analyser, respectively (Figure S3c and d in the revised SI). Scatter plots of those comparisons show Pearson coefficients > 0.84, and respective slopes of 0.83 and 1.10, supporting that CE = 0.6 for rBC is a reasonable CE correction approach. The following sentences and Figures S3 have been added to the revised manuscript and SI based on the above observations:

Page 2 lines 7-9: "Other co-located instruments for $PM_{2.5}$ characterizations include an aethalometer (AE33, Magee Scientific), a Monitor for Aerosols and Gases (MARGA, Metrohm) and a semi-continuous organic and elemental carbon (OC/EC) analyser (Sunset Laboratory)."

Page 4 lines 27-29: "The campaign averages of RIE_{rBC} and RIE_{NH4} were 0.15 (±0.04) and 4.24 (±0.04), respectively. The default RIE values of nitrate (1.1), sulfate (1.2) and organics (1.4) were used for respective mass concentration quantification (Jimenez, 2003)."

Page 4 lines 33-38: "The SP-AMS measurements were compared with the sulfate and OM concentrations measured by the MARGA and the OC/EC analyser, respectively, showing strong temporal (r = 0.77 and 0.93) and quantitative (slopes = 0.81 and 0.88) agreements between these measurements (Figure S3a and b). A collection efficiency (CE) of 0.6 was used for rBC quantification

due to incomplete overlap between the laser vaporizer and the particle beam (Willis et al., 2014). The corrected rBC concentrations were also comparable to those measured by the aethalometer (r = 0.96, slope = 0.83) and the EC measured by the OC/EC analyser (r = 0.84, slope = 1.1) (Figure S3c and d)."

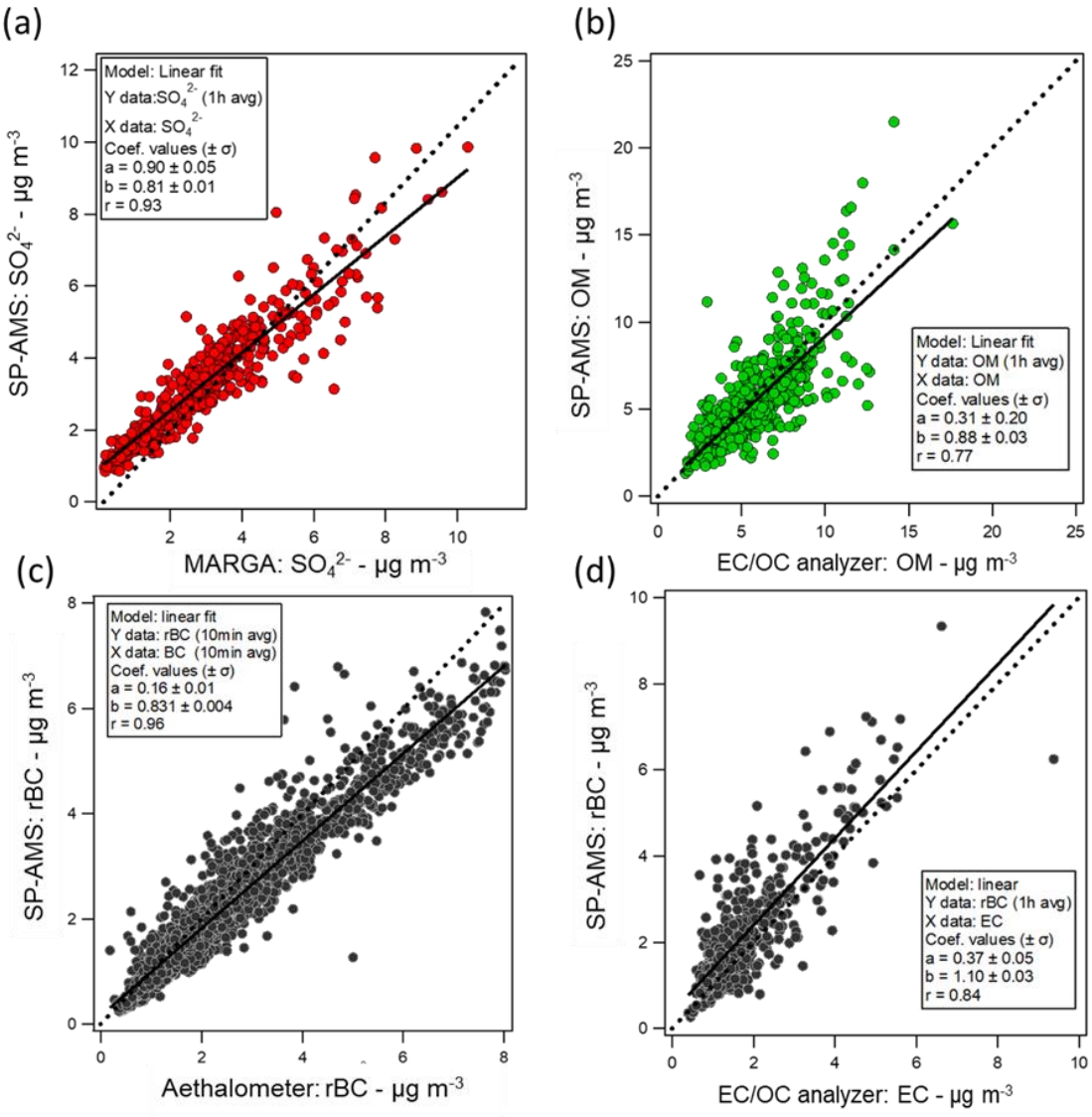

Figure S3: Scatter plots of (a) the hourly-averaged SO_4^{2-} mass concentration measured by the SP-AMS and MARGA, (b) and the hourly-averaged OA and OM (estimated from OC concentration using a 2.2 conversion factor) mass concentrations measured by the SP-AMS and OC/EC analyser, respectively. Comparisons of 10-min averaged rBC mass concentrations measured by the SP-AMS with (c) BC and (d) EC mass concentrations measured by the aethalometer and OC/EC analyser, respectively.

We agree with the reviewer that having the knowledge of coating and morphology of the BC-containing particles would be useful in determining the time-dependent CDCE of rBC measurements. However, the SP-AMS configuration used in this study (i.e., dual vaporization scheme) cannot provide further information on coating thickness and rBC morphology. Note that there is no standard approach for determining CDCE of rBC measured by the SP-AMS within the scientific community. In this work, we determined the CDCE of rBC by comparing BC (denoted as BC_{AE33} here after) and EC measured by the aethalometer and the OC/EC analyser, respectively. Comparisons between mass concentrations of our CE-corrected rBC ($rBC_{CE=0.6}$) with BC_{AE33} and EC give good Pearson coefficients of 0.96 and 0.71

and slopes of 0.83 and 1.10, respectively (Figure S3c and d). The histogram of CDCE determined for rBC using the two co-located instruments are reported in Figure S2b and c. The logarithmic distributions are centred on ~0.52 (±0.18) for aethalometer-based CDCE ($CDCE_{AE33}$) and 0.69 (±0.34) for OC/EC-based CDCE ($CDCE_{ECOC}$). These results are in a good agreement with the average CE value of 0.6 suggested by Willis et al., (2014) based on laboratory investigation.

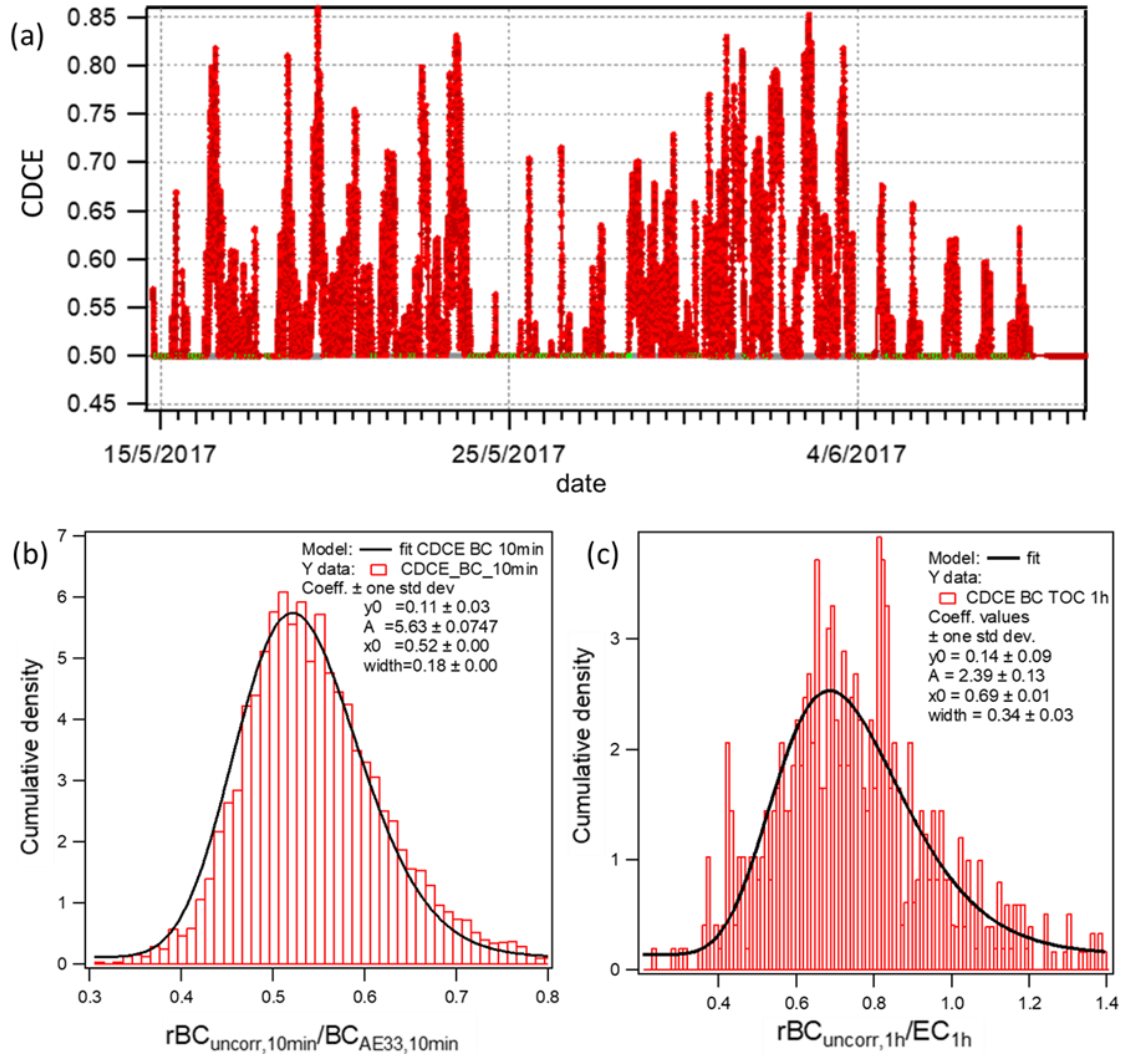

Figure S2: (a) Time series of composition-dependent collection efficiency ($CDCE_{Mid}$) determined over the entire campaign. Cumulative frequency of (b) aethalometer-based CDCE and (c) OC/EC-based CDCE, and their respective lognormal fitting determined over the entire campaign (with the fitting parameters corresponding to the following equation: $Y = y_0 + A \exp\left\{-\left[\frac{\ln(x/x_0)}{width}\right]^2\right\}$).

To evaluate the potential impact of CDCE of rBC and OA on our PMF results, three additional PMF analysis were performed by applying CDCE for rBC and/or OA, while other PMF setting remains unchanged. The metal ion signals were corrected to nitrate equivalent mass concentrations by assuming their RIE values equal to 1.

- Laser-off OA corrected by CDCE that were calculated based on the approach described by Middlebrook et al., (2012) ($CDCE_{Mid}$)

- Laser-on $CDCE_{Mid}$-corrected OA and $CDCE_{AE33}$-corrected C_n^+
- Laser-on $CDCE_{Mid}$-corrected OA and $CDCE_{AE33}$-corrected C_n^+ and metal ions

Comparisons between the CDCE-corrected results and the corresponding base cases reported in the main text (i.e., laser-off OA, laser-on OA + C_n^+ and laser-on OA + C_n^+ + metals) are shown in Table S4. Note that all PMF runs lead to five-factor solution (i.e., HOA, O-HOA, COA, LO-OOA and MO-OOA). Below is the brief summary of some major changes:

- OA fragments as PMF input: The time series of OA factors determined with $CDCE_{Mid}$ applied are similar to those without correction (i.e., Pearson coefficients > 0.91). Applying $CDCE_{Mid}$ correction result in 19-27% changes in the mass concentrations of each factor.

- OA, rBC and metals as PMF input: These modifications of PMF input do not make significant impacts on the relative contribution of each factor to the total OA and rBC. Except for the HOA factor, its contribution to the total rBC mass decreased from 44% to 33%. The C_1^+/C_3^+ ratios for MO-OOA are much more sensitive to CDCE corrections (i.e., increased from. 0.29-0.54 to 1.57-1.67) compared to other PMF factors. Even without applying CDCE correction, the C_1^+/C_3^+ ratios for MO-OOA varied between 0.29 and 0.54. Due to such large variations between cases, in addition to COA, no C_1^+/C_3^+ ratios were reported for MO-OOA in the main text.

- The CDCE corrections can affect the contributions of the five metals from each PMF factor to their total signals as shown in Table 1. The changes in the contributions of sodium and nickel from the LO-OOA and HOA factors to their total signals are relatively large compared to other metals and OA factors. It is important to emphasise that a few key observations remain unchanged: (1) K^+ and Rb^+ are strongly associated with MO-OOA, (2) V^+ is mainly associated with LO-OOA, and (3) Na^+ is associated with a few OA factors that are related to combustion emissions (i.e., LO-OOA, O-HOA, and HOA).

Overall, applying CDCE corrections for OA, rBC and metals do not result in substantial changes in our interpretations for most of the key observations. The discussion and conclusion developed based on the distribution of metals to different OA factors remains unchanged. Therefore, the original PMF results are used as a base case in our discussion in the main text. Table 1 shows the possible ranges of different parameters based on the results obtained from the CDCE-corrected PMF analysis. Table S4 summarizes the results of pre- and post-CDCE-corrected PMF analysis (Pre-CDCE: PMF solution obtained by the CDCE-corrected input matrices, Post-CDCE: PMF solution corrected by CDCE).

The above information has been added to the supplementary information. The following sentences have been added in the revised experimental section so that the readers can follow the detail of PMF analysis and results.

Page 5, lines 34-37: "The time dependent collection efficiency (or CDCE) of rBC were determined based on the BC measured by the aethalometer (Figure S2b). Additional PMF analysis, with CDCE applied on the input matrix for both OA and refractory components, were conducted (see details in Text S1 of the supplementary information). The PMF results were compared with those obtained without CDCE applied on the input matrix as shown in Table 1 and S4."

Table 1: Top: Carbon fragment ratios observed by the laser-on measurement for each PMF factor. The underlined number represents the results with both rBC fragments and trace metal ions included as PMF input. Bottom: Contribution of each PMF factor to the total signal of specific metal ions. For the entire table, the values in parenthesis are the one obtained from PMF with CDCE-corrected input matrix (see details in Text S1 and Table S4 of the supplementary information).

PMF factors	**HOA**	**O-HOA**	**COA**	**LO-OOA**	**MO-OOA**
Carbon fragments ratios					
C_1^+/C_3^+	0.66 (0.63) 0.65 (0.62)	1.00 (0.90) 1.00 (0.89)	NA*	0.81 (0.88) 0.79 (0.85)	NA#
C_2^+/C_3^+	0.38 (0.39) 0.38 (0.39)	0.41 (0.40) 0.41 (0.40)	NA*	0.39 (0.41) 0.41 (0.40)	NA#
Contribution of each factor to the total signal of specific metal ions (fraction)					
Na^+	0.35 (0.22)	0.14 (0.17)	< 0.01 (< 0.01)	0.45 (0.58)	0.06 (0.03)
K^+	0.23 (0.23)	0.19 (0.18)	< 0.01 (< 0.01)	<0.01 (0.05)	0.58 (0.54)
V^+	0.21 (0.08)	0.09 (0.16)	< 0.01 (< 0.01)	0.70 (0.76)	< 0.01 (< 0.01)
Ni^+	0.38 (0.22)	0.20 (0.22)	< 0.01 (< 0.01)	0.29 (0.45)	0.13 (0.11)
Rb^+	0.15 (0.15)	0.19 (0.19)	< 0.01 (< 0.01)	<0.01 (0.01)	0.66 (0.65)

* None of the refractory C_n^+ fragments were associated with the COA factor

Large variations of C_n^+ fragment ratios between cases, hence the ratios were not reported for MO-OOA

Table S4: Comparisons of the PMF results obtained from different CDCE correction approach (Pre-CDCE: PMF solution obtained by the CDCE-corrected input matrices, Post-CDCE: PMF solution corrected by CDCE). The post-CDCE solutions represent the corresponding base cases reported in the main text, Figure 3, and Figure S4.

PMF factors	**LO-OOA**			**MO-OOA**			**COA**			**O-HOA**			**HOA**		
Laser status	OFF	ON		OFF	ON		OFF	ON		OFF	ON		OFF	ON	
Type of PMF	OA	+ C_n^+	+ C_n^++ metal	OA	+ C_n^+	+ C_n^++ metal	OA	+ C_n^+	+ C_n^++ metal	OA	+ C_n^+	+ C_n^++ metal	OA	+ C_n^+	+ C_n^++ metal
Contribution to total OA mass (%)															
Post-CDCE	10.4	12.6	13.1	32.1	24.5	26.7	11.7	14.6	15.4	26.4	22.2	22.0	19.4	23.7	22.8
Pre-CDCE	12.4	12.3	12.1	30.8	28.5	29.6	12.6	16.3	17.8	21.0	20.6	19.7	23.2	22.2	21.4
Contribution to total rBC mass (%)															
Post-CDCE	NA	29.2	30.1	NA	6.2	6.4	NA	1.3	1.4	NA	20.1	20.7	NA	43.1	44.4
Pre-CDCE	NA	29.9	31.5	NA	7.4	8.8	NA	1.8	2.3	NA	26.5	24.4	NA	34.4	33.0
C_1^+/C_3^+															
Post-CDCE	NA	0.81	0.79	NA	0.54	0.29	NA	NA	NA	NA	1.00	1.00	NA	0.66	0.65
Pre-CDCE	NA	0.88	0.85	NA	1.76	1.57	NA	NA	NA	NA	0.90	0.89	NA	0.63	0.62
Time series - correlation coefficient (r)															
Post- vs. Pre-CDCE	0.98	0.97	0.91	0.99	0.99	0.99	0.98	0.97	0.96	0.89	0.93	0.94	0.99	0.97	0.97
Time series – slope															
Post- vs. Pre-CDCE	1.17	1.06	1.06	0.96	0.99	1.09	1.07	0.86	0.83	0.81	1.05	1.11	1.27	1.04	1.10
Normalized mass spectra - correlation coefficient (r)															
Post- vs. Pre-CDCE	1.00	0.95	0.94	1.00	1.00	0.99	1.00	0.93	0.92	1.00	0.99	0.99	0.97	0.99	0.99

2) In Sect. 3.4, the C1/C3 analysis should include a discussion about how uncertainty in the contribution of C1+ from non-refractory organic aerosol affects the interpretation of the ratio, particularly since a constant C1/C3 ratio was used to as a correction factor (Sect. 2.2). It may be beneficial to investigate the ratio of other Cx ions (e.g., C4/C3) to provide insight into the possible contribution of organics to C1.

Author's response: The C_1^+/C_3^+ ratio of 0.625 is used to calculate the total rBC mass concentrations. However, this correction was not applied when generating the PMF matrix. Instead, we applied Wang et al (2018) method to obtain the refractory fraction of C_n^+ for individual OA factor (i.e., correcting total C_n^+ fragments obtained from laser-on PMF by subtracting the organic fraction of C_n^+ ions retrieved from laser-off PMF). The lower intensities of the C_4^+-C_9^+, relatively to C_1^+-C_3^+ ions, can be strongly affected by neighbouring peaks (e.g. C_4^+ and SO^+), hence we did not report their values in the manuscript. To make this information clear, the related sentence has been revised as following.

Page 5 line 21-24: "Note that the interference of non-refractory organic signals on refractory C_n^+ fragments were subtracted based on the method described in Wang et al. (2018), and hence the C_1^+ fragment was not corrected based on the C_3^+ fragment, in the PMF analysis."

3) Sect. 3.5.1 would be strengthened by a more detailed discussion regarding urban sources of metals and including more metals in the analysis.

Author's response: Same response as reviewer #1, it is important to include all the detectable metal signals in the PMF analysis if possible. However, we only reported metals with their average values higher than the limit of detection (Table S2) determined by the particle-free air to ensure the quality of our data analysis. Nickel is a marginal case but a large fraction of its signal remain above its detection limit for investigating the V+/Ni+ ratio. To make this point clear, we have revised the sentence as shown below.

Page 5 lines 24-25: "Lastly, five metal ions (K^+, Na^+, Ni^+, V^+, Rb^+) were included into the PMF model (Figure S4g-i) as the majority of their signals were higher than their respective limit of detection (Table S2)."

Furthermore, we have followed the recommendations from reviewer #1 to include more possible sources of metals, such as biomass burning emissions for Na^+ and coal combustion emissions for Rb^+, in our discussion. Below are a few sentences/paragraphs that we have modified. Please see more detail of modification in the revised version highlighted in the point-by-point responses to reviewer #1.

Page 12 lines 5-7: "Based on the PMF results that includes trace metal ions, sodium (Na^+) was mainly associated with HOA, O-HOA and LO-OOA (Figure 5a) that could be due to different types of fossil fuel combustion emissions (e.g., local traffic, shipping, and various industrial activities) as discussed in Section 3.4."

Page 12 lines 20-23: "Biomass burning can be a possible source of Na^+ (Hsu et al., 2011) but no major fresh biomass burning emissions were observed in this study. The MO-OOA factor is suspected to be more influenced by aged regional biomass burning emissions (see more discussion in Section 3.5.2) but Na^+ was not strongly associated with this factor."

Page 13, lines 27-30: "The regional origin of K^+, Rb^+, $C_2H_4O_2^+$ and MO-OOA were investigated through their PSCF. Their PSCF graphs (Figures 6d and S15a- c) show several common origins with high probability that the highest concentrations could be influenced by biomass burning events from Indonesia (Figure S12a). Nevertheless, coal-fired power plants are located nearby the identified

hotspots of Rb^+ and K^+ (Figure S12b) so that a regional transport of coal-fired power plant emissions alongside biomass burning plumes were possible".

Additionally, the potential contribution of oceanic sources to Na^+ should be discussed in more detail. While the authors state that Na+ and Cl- exhibit poor temporal correlation, I assume this is for the whole data set. If one filters by wind direction (and thus sea breeze) does this still hold? Additionally, is there an interpretation for the large contribution of Na+ in LO-OOA? Finally, does the fact that different C1/C3 ratios were seen for LO-OOA and HOA (the factors with the strongest Na+ contribution) tell us anything about the different sources of Na+?

Author's response: Thanks for the suggestion on the data analysis. Firstly, the comparison between Na^+ and Cl^- under sea breeze conditions do not improve the correlation, with $r < 0.1$ (n=3384). The large contribution of Na^+ in LO-OOA can be due to the fact that this OA factor is associated with industrial emissions. In particular, LO-OOA had the second largest contribution to the total rBC, suggesting that at least a fraction of rBC from industrial emissions could act as effective condensation sinks of LO-OOA produced via the photochemistry along their dispersion as discussed in Section 3.4 of the original manuscript. Finally, the different C_1^+/C_3^+ ratios between LO-OOA and HOA can provide insight to the possible sources of Na^+ as discussed in Sections 3.4 and 3.51. To better connect the two Sections, a sentence has been added in Section 3.5.1, and the paragraph in Section 3.4 has been revised as following.

Section 3.5.1, page 12, lines 5-7: "Based on the PMF results that includes trace metal ions, sodium (Na^+) was mainly associated with HOA, O-HOA and LO-OOA that could be due to different types of fossil fuel combustion emissions (e.g., local traffic, shipping, and various industrial activities) as discussed in Section 3.4."

Section 3.5.1, page 12, Lines 18-20: "However, it is important to emphasize that Na^+ and Cl^- exhibit rather poor temporal correlations ($r < 0.30$) for both laser-off and laser-on data regardless the influences of sea breeze."

Section 3.4, page 11, lines 13-27: "The C_1^+/C_3^+ ratios of rBC associated with HOA was 0.66 (±0.07) , which was within the range of those emitted from aircraft-turbine, regal black (i.e., a BC standard for SP-AMS calibration) and particles produced by a propane diffusion flame (0.50 – 0.78) and, more importantly, close to those reported for diesel engine exhaust (Carbone et al., 2019; Corbin et al., 2014; Onasch et al., 2012). Furthermore, the size distribution of unit mass resolution data shows lower *m/z* 12-to-*m/z* 36 ratios (a proxy for C_1^+/C_3^+) for particles with d_{va} smaller than 100 nm (Figure S11a). This suggests that rBC particles with relatively small diameter were mainly associated with fresh traffic emissions (Massoli et al., 2012). Our results illustrate that rBC transported from industrial area and shipping ports gave C_1^+/C_3^+ ratios closer to unity (i.e., LO-OOA = 0.79 (±0.10) and O-HOA = 1.00 (±0.11), which is similar to the previous observations for soot particles emitted from a marine engine using heavy-fuel-oil (Corbin et al., 2018), rBC-containing particles emitted from chemical and petrochemical industries (Wang et al., 2018), and rBC with high fullerene content (Canagaratna et al., 2015a; Corbin et al., 2014). The NWR and diurnal plots of C_1^+/C_3^+ ratio (Figure 4c and d) clearly show that rBC with higher C_1^+/C_3^+ ratios were transported to the site by sea breeze from the southwest direction, which are consistent with our PMF results that O-HOA and LO-OOA were influenced by industrial emissions and were associated with rBC with higher C_1^+/C_3^+ ratios compared to other OA components."

4) To me, it seems that the last sentence of the introduction and the last paragraph of the conclusions overstate the implications and applications of the manuscript. Optical properties of aerosols were not

discussed in the manuscript, so the inclusion in the introduction and conclusion seems out of place. Moreover, the work of Kasthuriarachchi et al (2019) is under review so the inclusion here is somewhat misleading. I suggest that the authors consider revising this paragraph and the last sentence of the introduction to better reflect the material covered in this study.

Author's response: The last sentence of the introduction has been removed as suggested. In addition, the last paragraph of conclusion has been revised as following. In particular, the observations from Kasthuriarachchi et al (2020) has been removed from the conclusion.

Page 14, lines 37-38 to Page 15, lines 1-9: "More broadly, the improved source identification for OA and rBC can provide useful information to further investigate the effects of atmospheric aging on their physio-chemical properties. For example, this work highlights the potential influences of regional biomass burning and coal combustion emissions to MO-OOA component, which may provide important insight into how light absorbing properties of OA (i.e., brown carbon) evolve with transport and aging. Recently, Dasari et al. (2019) provided field evidence for the bleaching of brown carbon during their transport by photo-oxidation and that photo-dissociation can occur in the South Asian outflow based on measurements near and away from specific combustion sources, including biomass burning and traffic. Furthermore, this type of PMF analysis could be applied to analyze the sources and characteristics of rBC-containing particles exclusively (i.e., rBC core with organic coatings) in order to advance our understanding on the effects of primary emissions and/or atmospheric processing on BC light absorption enhancement caused by the lensing effect."

Minor comments

-It would be helpful to explicitly pinpoint some of the main industrial sources (such as the oil refinery discussed in the introduction and shipping ports) in Figure S1a.

Authors' response: The major industrial activities occurring on Jurong Island (i.e., an industrial zone located at the southwest direction of sampling site) have been added in Table S1. Additional pins have been added to illustrate their locations in Figure S1a.

-Page 7 lines 12-15: Regarding the production of organo-sulfur compounds in acidic sulfate plumes – this seems rather poorly supported at the moment. As it does not advance the main focus of the paper, I suggest removing. -Figure S4a the legend (colours based on CH2SO) does not match the caption (data originating from SW and other directions).

Authors' response: We agree with the reviewer and have removed the sentence regarding the production of organo-sulfur compounds in acidic sulfate plumes. The caption has been corrected to match the figure (Figure S6 in the revised version).

-Figure S4d needs a color scale. The 2 modes (discussed at the end of page 6) are also not apparent from this figure, perhaps due to the color scale used. Currently it looks to me more like the distribution broadens when the concentration increases in the middle of the day.

Authors' response: The colour scale has been added to Figure S6a (former Figure S4d). We agree with the reviewer that the distribution of sulfate particles broaden in the middle of the day. It is worth noting that the Figure S6a is the average of the entire campaign. If we separate the strong sulfate plumes from

the entire dataset, Figure S6d (former Figure S4b) shows that the sulfate particles size is smaller for the strong sulfate plumes compared to the rest of periods. The sentences have been revised as following.

Page 7, lines 21-26: "This particle acidity dependence seems to coincide with diurnal variations of SO_4^{2-} size distribution. Throughout the day, relatively large sulfate particles are observed with their vacuum aerodynamic diameter (d_{va}) peaked at ~400 nm, whereas those encountered during the sea breeze present a broader mode with d_{va} ranging between 200 and 400 nm (Figure S6a and d). This suggests that a large fraction of acidic SO_4^{2-} particles observed during the sea breeze period were freshly formed in the atmosphere."

-Discuss figures in order (e.g., Fig. S6 is currently referenced before S5). Cite panels of figures in order (for instance, the panels of Fig. S4 are cited out of order).

Authors' response: Both manuscript and SI figures have been re-arranged accordingly.

-Figure S5: The wording in the caption is unclear, specifically "... both filtered from 25th to 28th of May, over the campaign." Is "both" just COA and HOA? Does it mean that only the 25th to 28th was included?

Authors' response: We agree with the reviewer and have reworded the caption as follow:

Figure S8 (former Figure S5): "Figure S8: Diurnal cycles of (a) N:C (laser-off mode), (b) NO_x, (c) CO, (d) COA, (e) HOA, and (f) O_3 over the campaign. The plain and dotted lines represent the medians and averages values, respectively. The shaded regions represent the 25th and 75th percentiles. Note that data between May 25th to 28th were excluded for HOA and COA due to the strong unknown emission during the nighttime."

-In Sect 3.5.2, why use m/z 60 rather than the HR ion (C2H4O2+)?

Authors' response: The f_{60} was calculated using organic fragment signals at $C_2H_4O_2^+$. We have replaced f_{60} and m/z 60 by $f_{C2H4O2+}$ and m/z $C_2H_4O_2^+$, respectively, in Section 3.5.2 and corresponding figures.

-Page 10 line 27: rather than "inferior" use "smaller than"

Authors' response: The correction has been made.

-Page 12 line 23: I do not find the similar size distributions for m/z 39 and 60 to be convincing evidence for a BBOA source. m/z 60 is the only individual organic ion shown in Fig. S8b. How unique is the size distribution for m/z 60 compared to other individual organic ions?

Authors' response: We agree with the reviewer so that the sentence has been removed. However, we have decided to keep the Figure in SI as literature information.

-Page 12 line 19: should this be Figure 5d rather than 3c and 4b?

Authors' response: We thank the reviewer for pointing out this error. It has been corrected in the revised version.

References:

Canagaratna, M. R., Massoli, P., Browne, E. C., Franklin, J. P., Wilson, K. R., Onasch, T. B., Kirchstetter, T. W., Fortner, E. C., Kolb, C. E., Jayne, J. T., Kroll, J. H. and Worsnop, D. R.: Chemical Compositions of Black Carbon Particle Cores and Coatings via Soot Particle Aerosol Mass Spectrometry with Photoionization and Electron Ionization, J. Phys. Chem. A, 119(19), 4589–4599, doi:10.1021/jp510711u, 2015.

Carbone, S., Timonen, H. J., Rostedt, A., Happonen, M., Rönkkö, T., Keskinen, J., Ristimaki, J., Korpi, H., Artaxo, P., Canagaratna, M., Worsnop, D., Canonaco, F., Prévôt, A. S. H., Hillamo, R. and Saarikoski, S.: Distinguishing fuel and lubricating oil combustion products in diesel engine exhaust particles, Aerosol Sci. Technol., 0(0), 1–14, doi:10.1080/02786826.2019.1584389, 2019.

Corbin, J. C., Sierau, B., Gysel, M., Laborde, M., Keller, A., Kim, J., Petzold, A., Onasch, T. B., Lohmann, U. and Mensah, A. A.: Mass spectrometry of refractory black carbon particles from six sources: carbon-cluster and oxygenated ions, Atmos Chem Phys, 14(5), 2591–2603, doi:10.5194/acp-14-2591-2014, 2014.

Corbin, J. C., Mensah, A. A., Pieber, S. M., Orasche, J., Michalke, B., Zanatta, M., Czech, H., Massabò, D., Buatier de Mongeot, F., Mennucci, C., El Haddad, I., Kumar, N. K., Stengel, B., Huang, Y., Zimmermann, R., Prévôt, A. S. H. and Gysel, M.: Trace Metals in Soot and PM $_{2.5}$ from Heavy-Fuel-Oil Combustion in a Marine Engine, Environ. Sci. Technol., 52(11), 6714–6722, doi:10.1021/acs.est.8b01764, 2018.

Dasari, S., Andersson, A., Bikkina, S., Holmstrand, H., Budhavant, K., Satheesh, S., Asmi, E., Kesti, J., Backman, J., Salam, A., Bisht, D. S., Tiwari, S., Hameed, Z. and Gustafsson, Ö.: Photochemical degradation affects the light absorption of water-soluble brown carbon in the South Asian outflow, Sci. Adv., 5(1), eaau8066, doi:10.1126/sciadv.aau8066, 2019.

Hsu, L.-J., Alwahabi, Z. T., Nathan, G. J., Li, Y., Li, Z. S. and Aldén, M.: Sodium and Potassium Released from Burning Particles of Brown Coal and Pine Wood in a Laminar Premixed Methane Flame Using Quantitative Laser-Induced Breakdown Spectroscopy:, Appl. Spectrosc., doi:10.1366/10-06108, 2011.

Jimenez, J. L.: Ambient aerosol sampling using the Aerodyne Aerosol Mass Spectrometer, J. Geophys. Res., 108(D7), doi:10.1029/2001JD001213, 2003.

Massoli, P., Fortner, E. C., Canagaratna, M. R., Williams, L. R., Zhang, Q., Sun, Y., Schwab, J. J., Trimborn, A., Onasch, T. B., Demerjian, K. L., Kolb, C. E., Worsnop, D. R. and Jayne, J. T.: Pollution Gradients and Chemical Characterization of Particulate Matter from Vehicular Traffic near Major Roadways: Results from the 2009 Queens College Air Quality Study in NYC, Aerosol Sci. Technol., 46(11), 1201–1218, doi:10.1080/02786826.2012.701784, 2012.

Middlebrook, A. M., Bahreini, R., Jimenez, J. L. and Canagaratna, M. R.: Evaluation of Composition-Dependent Collection Efficiencies for the Aerodyne Aerosol Mass Spectrometer using Field Data, Aerosol Sci. Technol., 46(3), 258–271, doi:10.1080/02786826.2011.620041, 2012.

Onasch, T. B., Trimborn, A., Fortner, E. C., Jayne, J. T., Kok, G. L., Williams, L. R., Davidovits, P. and Worsnop, D. R.: Soot Particle Aerosol Mass Spectrometer: Development, Validation, and Initial Application, Aerosol Sci. Technol., 46(7), 804–817, doi:10.1080/02786826.2012.663948, 2012.

Wang, J., Wu, Y., Ge, X., Shen, Y., Ge, S. and Chen, M.: Characteristics and sources of ambient refractory black carbon aerosols: Insights from soot particle aerosol mass spectrometer, Atmos. Environ., 185, 147–152, doi:10.1016/j.atmosenv.2018.05.011, 2018.

Willis, M. D., Lee, A. K. Y., Onasch, T. B., Fortner, E. C., Williams, L. R., Lambe, A. T., Worsnop, D. R. and Abbatt, J. P. D.: Collection efficiency of the soot-particle aerosol mass spectrometer (SP-AMS) for internally mixed particulate black carbon, Atmos Meas Tech, 7(12), 4507–4516, doi:10.5194/amt-7-4507-2014, 2014.